# Thermographic and Fractographic Analysis of the Heat Treatments Effect on Al 6061-T6 Fatigue Life

Víctor I. Rodríguez-Reyes, Kevin Edson Petatan Bahena, Arturo Abúndez-Pliego and Benjamín González Vizcarra



November 22, 2023

# Thermographic and fractographic analysis of the heat treatments effect on Al 6061-T6 fatigue life

**Víctor I. Rodríguez-Reyes** * **Kevin Edson Petatan Bahena** *
**Arturo Abúndez-Pliego** * **Benjamín González Vizcarra** **

* *Tecnológico Nacional de México / CENIDET, Av. Palmira Esq. Apatzingán S/N, Col. Palmira. C.P. 62490, Cuernavaca. Morelos, México (e-mail: victor.rodriguez18me@cenidet.edu.mx, d20ce008@cenidet.tecnm.mx, arturo.ap@cenidet.tecnm.mx).*
** *Universidad Autónoma de Baja California / FCITEC, Blvd. Universitario No. 1000, Unidad Valle de las Palmas. C.P. 21500. Tijuana, B.C. México (e-mail: bgonzalez79@uabc.edu.mx)*

**Abstract:** In this work, a qualitative assessment of the influence of heat treatments sequence on Al6061-T6 fatigue behavior was performed. The aluminum alloy was, on one hand, subjected to a set of designed heat treatments of aging, retrogression and reageing and then tested in a rotating beam fatigue machine; on the other hand, temperature evolution of specimens under fully reversed rotating beam cyclic loading was measured through an infrared thermographic camera. The evolution of temperature and its relationship with the fatigue life was discussed. Factographies were done as a complement in order to have visual evidence of the effect of the heat treatments on the nucleation and propagation of the fatigue crack. Evidence of the relationship between the fracture crack growth and the steady-state temperature of the tests was observed.

*Keywords:* heat treatments, aluminum, rotating bending, fatigue life, infrared thermography, fractography

## 1. INTRODUCTION

Fatigue failure is a phenomenon which consists in the presence of cracks and deformations generated by cyclic loading, which eventually lead to a failure by fracture, even when loading does not surpass the elastic limit. The costs associated with fractured materials can reach up to 4% of the gross domestic product (Reed et al., 1983). It has been related to many failures and disasters in many industries as aviation, oil and gas, railway transport, among others (Schütz, 1996). Only in the railway industry, one of the most remarkable disasters was the Versailles rail accident in 1842, due to a broken axle which failed by fatigue. Then, metal fatigue was poorly understood, and this led to August Wöhler to research this phenomenon and to propose the now known S-N curves. In 1998, the Eschede train disaster was caused by a fatigue crack in one wheel with poor design. In 2021, Mexico City Metro overpass collapse was caused, among other things, by the lack of functional studs and poor-quality welds that led to fatigue. As can be seen by the cases mentioned above, fatigue failure still has much incidence and, since currently there are many projects in railway industry such as Mayan Train, Interurban Train Mexico City–Toluca and the Interoceanic Corridor of the Isthmus of Tehuantepec, it is important to keep researching this type of failure, in order to saving costs and avoiding disasters with human fatalities.

Heat treatments consist in the modification of the mechanical properties and metallographic structure of the material by controlled increases and decreases of temperature. They are applied for improving the performance of materials, through forming precipitates within the material, being an impediment for the motion of dislocations, increasing the elastic limit and the ultimate strength. Therefore, heat treatments are a reliable tool for improving fatigue life of aluminum alloys. Heat treatments of retrogression and reageing increase the rigidity of the material and decrease the fatigue crack growth rate, improving the properties of damage tolerance (Abúndez et al., 2016; Mayén et al., 2019). Heat treatments also increase the elastic and endurance limit (Mayen et al., 2019; Nelaturu et al., 2020). On the contrary, even when heat treatments improve the mechanical properties of the material and its behavior in low-cycle fatigue, they can decrease the resistance to plastic strain, reducing the ductility of the material and making it to behave brittle (Azadi and Shirazabad, 2013).

The relation between fatigue life and energy dissipation has been of interest for many researchers, as recent literature shows (Teng, 2023). Naderi et al. (2010) calculated the entropy generation of metallic materials under cyclic loading by integrating the energy dissipation over the material temperature along the fatigue tests. They proposed the hypothesis that entropy generation at the point of fracture is constant and independent of the stress level, loading frequency and geometry of the specimen, being a material parameter. They named this concept as fracture fatigue entropy (FFE). Based on this hypothesis, a series of methodologies for prevention of failures in metallic materials under cyclic loadings have been developed (Naderi and Khonsari, 2011; Teng, 2023). They are based on the measurement of temperature evolution during the fatigue tests, which can be done with infrared thermography, having the advantage of being a noncontact and nondestructive technique. It has been shown that, when a material is subjected to constant amplitude cyclic loading, it presents dissipation of energy, which manifest itself as heat. This heat is manifested as a temperature evolution, characterized by three stages, which are related to the stress-strain response: an initial rapid temperature increase, a steady-state temperature during a large part of the fatigue process, and a final abrupt temperature increase, followed by a drop after the failure. Therefore, the change of temperature during fatigue can be used as an index of accumulation of damage for fatigue life prediction.

In this work, Al 6061-T6 is subjected to heat treatments of own design in order to find the best combination of temperature and time treatment which improves the fatigue life, tested under constant amplitude loading. The temperature behavior of the material was monitored, and fractographies were done, in order to determine the influence of the heat treatment and to determine how the crack propagation rate changes according to each one, by the effect of the precipitation of the solid phases.

## 2. EXPERIMENTAL PROCEDURE

The number and geometry of specimens were proposed according to the ASTM E739 (ASTM International, 2004) and ASTM E466 (ASTM International, 2002) standards, respectively. The specimen geometry is shown in Fig. 1, where the diameter $d$ of the gage length is 6.35 mm (1/4 in).

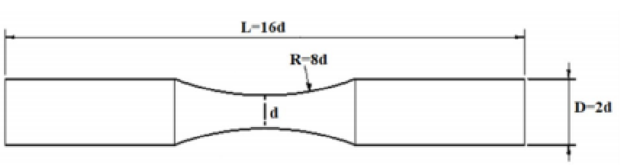


Fig. 1. Geometry of the specimens in function of the diameter d of the gage section, according to ASTME466.

The material selected is Al 6061-T6, its chemical composition and mechanical properties are shown in Table 1 and Table 2, respectively.

Six different levels of time and temperature for the heat treatments were proposed, with six samples for each treatment. The total number of specimens for the fatigue tests were 72. The defined sequence for the treatments consists in (1) a solution at 554 °C for one hour, (2) immediate cooling of the specimens in water at room temperature, (3) artificial reageing in the designed conditions of temperature and time for the designed heat treatments and finally (4) a retrogression at 250 °C for 10 minutes. The parametric design for the heat treatments is shown in Table 3.

### *2.1 Experimental setup*

The used fatigue testing apparatus is a rotating beam fatigue test machine with a constant-speed motor of 1740 rpm (29 Hz). Tests include clamping the specimen at both ends in grips, and dead weight makes the load to fluctuate between tension and compression at a specified stress amplitude of 150 MPa, being completely reversed load. All tests were conducted by setting up a pristine sample in the machine and continuously running until fracture. Infrared thermography was used to acquire the temperature of the specimens during the fatigue tests. Hti HT-18 camera was used for capturing thermal images from the specimen every five seconds. Before the experiment, the specimen surface was painted with a black mate color to increase the thermal emissivity and thus enhance the temperature measurement accuracy. Fig. 2 shows thermal images of a specimen before and halfway through a test. The temperature evolution of the specimen is quite clear.

About a possible error scattering in the temperature measurement, it is feasible that some unconsidered and uncontrolled variables may affect the measuring. Such variables may be the ambient temperature, lightning (heat transfer by radiation), air currents (heat transfer by convection), incorrect assembly (mechanical unbalances), among others. Then, a proper energy balance should be solved to know the amount of each heat component, although some researches have shown that heat transfer may be considered negligible if it is not part of the parametric study (Naderi et al., 2010). Besides, in order to make the mentioned characterization, some physical properties are necessary, which were not estimated in this study.

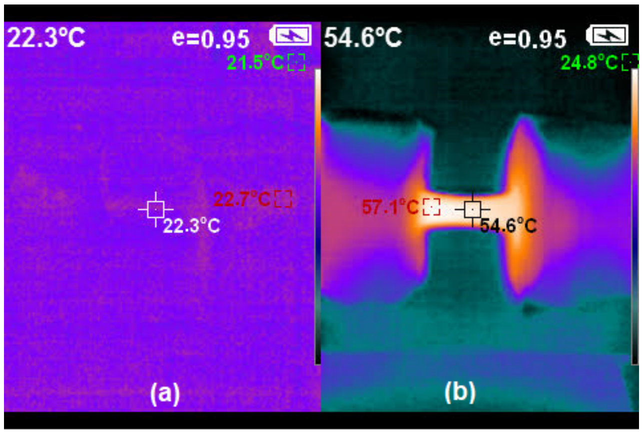


Fig. 2. Thermal image of the specimen (a) before and (b) halfway through a fatigue test.

Visual inspection of the fracture surfaces was conducted using a Mitutoyo Stereo Microscope, with 20x magnification. Photographies were taken with a True Chrome II camera.

## 3. RESULTS AND DISCUSSION

Results such as fatigue life, a statistical analysis of the dispersion of the data, a regression model between fatigue life and the parametric conditions of the designed heat treatments, and the energy required for each of them can be consulted in reference: (Petatan Bahena, 2022).

Table 1. Component elements (% by weight).

| Alloy | Al | Cr | Cu | Fe | Mg | Mn | Si | Ti | Zn | Other |
|---|---|---|---|---|---|---|---|---|---|---|
| 6061-T6 | 95.8-98.6 | 0.04-0.35 | 0.15-0.40 | <=0.70 | 0.80-1.2 | <=0.15 | 0.40-0.80 | <=0.15 | <=0.25 | <=0.15 |

Table 2. Mechanical properties.

| Ultimate Tensile Strength | Yield Tensile Strength | Elongation at break (%) | Modulus of elasticity (GPa) | Poisson's ratio | Fatigue Strength (MPa) | Shear modulus (GPa) | Shear Strength (MPa) |
|---|---|---|---|---|---|---|---|
| 310 | 276 | 17 | 68.9 | 0.33 | 96.5 | 26 | 207 |

Table 3. Heat treatments in function of temperature and time.

| Condition | Temperature (ºC) | Time (minutes) |
|---|---|---|
| T1 | 150 | 120 |
| T2 | 165 | |
| T3 | 180 | |
| T4 | 195 | |
| T5 | 210 | |
| T6 | 225 | |
| C1 | 192 | 30 |
| C2 | | 60 |
| C3 | | 90 |
| C4 | | 120 |
| C5 | | 150 |
| C6 | | 180 |

Here only the results from infrared thermography and fractography are being presented and discussed.

### *3.1 Thermographic analysis*

The temperature behavior of the specimens under fatigue tests until fracture are depicted in Fig. 3, where it is possible to observe that all exhibited a similar behavior of three well-identified phases. In the first phase, the temperature increases rapidly. The second phase begins when the temperature stabilizes and becomes constant. The third and last phase occurs rapidly before failure, when the temperature suddenly rises. The third phase occurs very fast, so the infrared camera is unable to record most of the temperature evolution in this part of the tests. In the figure, OO represents the material without thermal treatment.

The different initial temperature slopes of the samples are associated with its capacity to dissipate energy, as some researches have shown (Teng, 2023). It is usual to use the temperature slope to characterize the dissipation of energy of a fatigue process, although the density of the material and its heat capacity are required. While the density among the material without the heat treatments and the treated samples should be the same, the heat capacity must have changed, as the change in the temperature rate shows.

The heating is mainly caused by the plastic deformation of the material, if there are not external heat sources. In this case, the specimens were tested at room temperature without controlling temperature or air fluxes, although they were not study variables, so their influence were considered as negligible. On the other hand, temperature is a frequency dependent parameter, then testing the material to higher frequencies would elevate the temperature rate, and vice versa for low frequencies. Since this study was conducted to a constant frequency, the influence of this parameter in the temperature evolution can be considered negligible too.

The temperature plateau reached by many of the tested specimens is explained by the process of work hardening of the material, caused by the dislocations movement and generation at the beginning of the fatigue process. Then, a resistance to deformation is developed, which causes a constant hysteretic behavior in the associated stress-strain curve, and this behavior is exhibited in the reached steady state temperature.

It can be seen that some specimens do not present a steady-state temperature (phase II). Specifically, heat treatments OO, T1, T6, C1 . This can be related to the short fatigue life, compared with heat treatment T4, for example, being the one that achieved the largest extension of fatigue life. This only can mean that the heat treatment T4 must have changed some microstructural properties which decrease the microstructural plastic deformation and therefore the energy dissipation exhibited as heat, since some characteristics like the elastic deformation or internal friction produce only the variation of the temperature around a mean, and not the temperature increase.

### *3.2 Fractographic analysis*

In the following images of the fractured surfaces obtained by microscope, the fracture mechanisms can be observed. It can be seen diverse points where the crack started, which progressed until fracture. They propagate in a stable regime through the interior of the material until fracture. With the scale of these fractographies, it is not possible to perceive benchmarks totally, although the duration of the crack propagation can be qualitatively inferred.

In Fig. 4 a fractography image of one specimen without heat treatment is shown. It can be seen that the crack nucleation occurred in multiple zones of the specimen, as shown by the yellow lines, from where the crack propagation extended through the red circle, as the Chevron marks shown as purple lines. The figure shows that a brittle fracture (plane zone delimited by the red circle) is extended up to 90% of the total fracture surface. The final fracture occurred at the zone represented by the green line, where protuberances at 45º can be appreciated, which are typical characteristics of a ductile fracture.

In Fig. 5 similar patterns can be seen for a specimen with treatment T4, the one which achieved the longest life. A 100% ductile fracture zone is evidenced by the

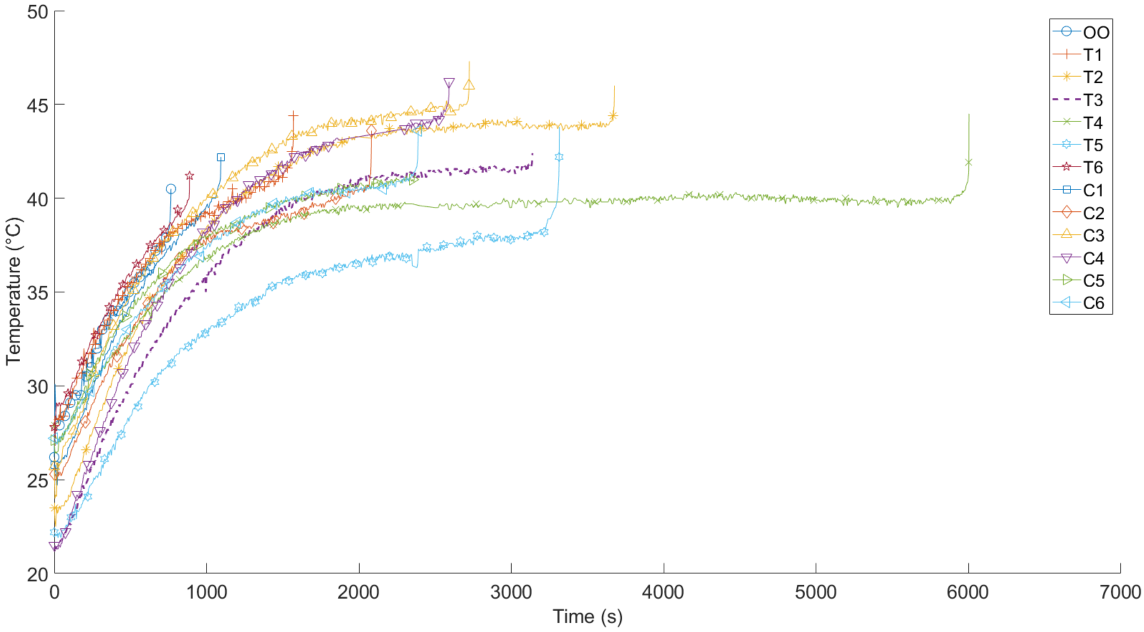


Fig. 3. Temperature variation in the rotating beam fatigue test of Al6061-T6 specimens at 150 MPa. OO denotes specimen without treatment.

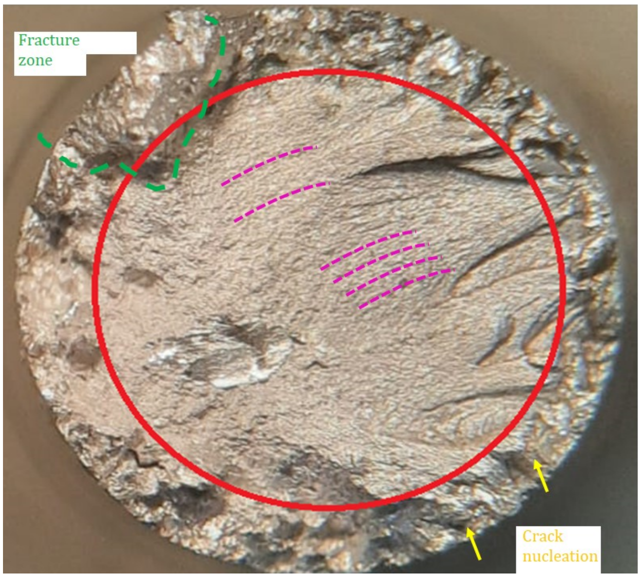


Fig. 4. Plane fracture surface of a failured specimen without thermal treatment.

protuberances at 45º (see the green line). Multiple crack nucleations can be appreciated too and the crack propagation is evidenced by the Chevron marks pointed by the purple lines. The crack propagation zone is smaller than the one of a specimen without treatment. This is a clear sign that the crack propagation had an extended duration since the heat treatment must had improved the strength of the material to fatigue stresses.

The changes between Fig. 5 and Fig. 4 may indicate a decrease on the acting stress, or an increment of the strength of the material. The crack propagation area in Fig. 4 is centered on the plane fractured surface of the specimen, which indicates that the specimen was subjected to higher nominal stresses than the specimen of Fig. 5. In this last one, the crack propagation area is lightly displaced from the center of the specimen, in opposite direction of the rotation, which is a characteristic of fractures occurring under rotating bending load, being more evident under low nominal stresses.

Among other factors which can influence in the change of the fracture behavior seen in the fractographies are local microstructure differences, variation of the medium

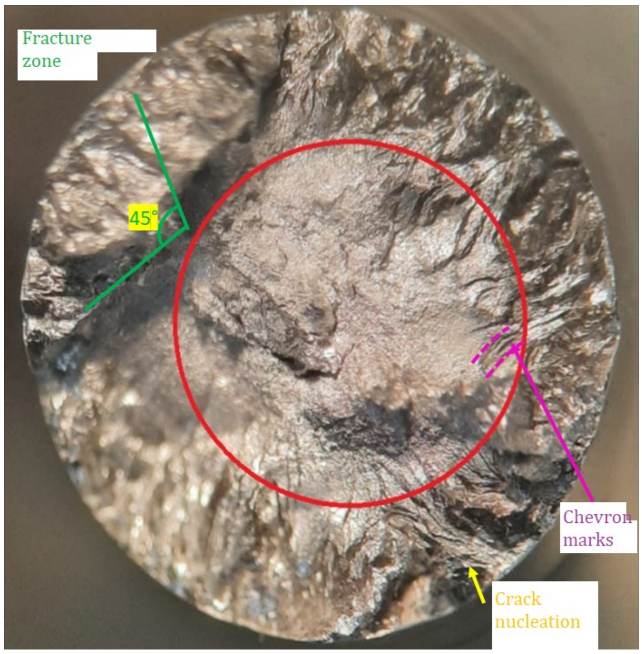


Fig. 5. Ductile fracture surface of a failured T4 specimen.

in which the crack propagates, local variations in the state of stress, etc., which may be influenced by the heat treatments.

Finally, in Fig. 6 the fractography of a C1 specimen can be seen. A mixed fracture surface, delimited by the red circle, can be seen, with an extension up to 70% of the area, and the final ductile fracture zone is associated with the protuberances at 45º (see green line), with an extension up to 30% of the area. The specimen showed multiple crack nucleation points (yellow arrows), from where the crack propagated, as can be seen by the Chevron marks (purple lines). Heat treatment C1 barely improved the fatigue life of the AA6061-T6. Besides, the thermal behavior of the specimens showed a continuous change in temperature rate, not allowing to reach a steady-state temperature.

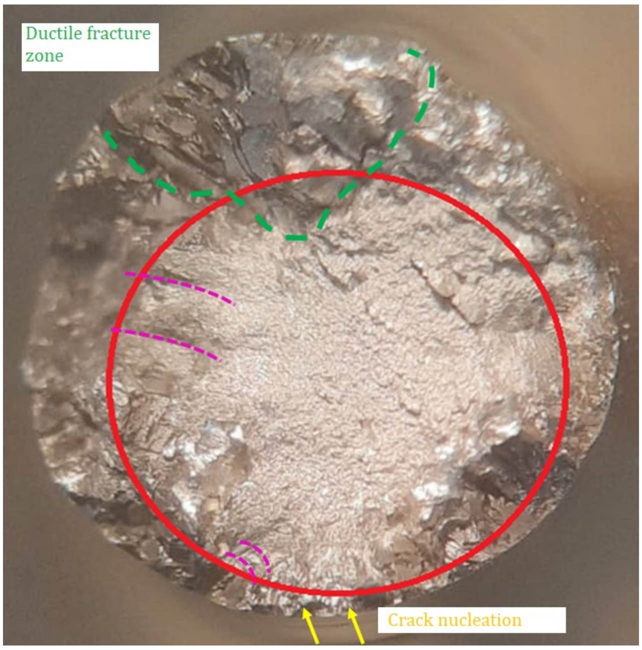


Fig. 6. Mixed Fracture Surface of a failured C1 specimen.

It was found that temperature, rather than the time, has the highest influence aimed at improving the fatigue life, since its increment generates precipitates which increases ductility, as can be evidenced by the protuberances observed in fractographies. When a material reaches the equilibrium state, its entropy (and associated disorder) level is maximum. To increase orderliness, the material needs to deviate from equilibrium state. In a fatigue process, this can occur by self-organization, which is associated with the formation of dissipative structures. In a fatigue process, these dissipative structures correspond to the arrangement of new patterns of the material's microstructure, for example, a critical density of dislocations, particle size distribution, orientation of crystals, persistent slip bands, and thanks to them, the entropy generation in the system decreases, resulting in a slowing down of the fatigue damage and the increasing of fatigue life. As a result of self-organization, the material reaches a lower entropy generation after the heat treatment, compared to the thermodynamic state before the occurrence of dissipative structures. The concept of dissipative structures was presented by Nobel prize winner Prigogine (1978) and its use for the creation of more resistant materials has been discussed in references: (Khonsari and Amiri, 2012; Naderi, 2020).

## 4. CONCLUSION

An in-depth understanding of the conditions leading to the formation of dissipative structures and to self-organization in materials after heat treatments might lead researchers and engineers to improve and to design novel materials with longer useful life or better properties. Therefore, continuous research which tries to relate the effects of heat treatment processes with the modification of this dissipative structure in a quantitative form is required.

For now, the thermography and fractography at the scale done in this case study allows to relate the fatigue crack propagation and the steady-state temperature of the process in a qualitative form, being both evidence of the modification of the microstructure of the material, resulting in decreasing the rate of entropy generation and, therefore, slowing down the damage in the material and consequently increasing its useful life. That's why the quantification of this dissipative structures is necessary, in order to relate them to the parameters of the heat treatments. Then, the better combination of time and temperature for the heat treatments can be proposed in order to maximize the fatigue life, based on the physics of the process and not only with regression models from curve fitting.

A qualitative relation between temperature and the mode of failure was established. Treatment T4 exhibited a ductile failure and the measured temperature evolution depicted a steady-state temperature for a longer time. In contrast, treatment C1 showed a continuous increasing temperature and a mixed mode of failure. Although the size of the crack propagation areas would be important to be estimated, this work was bounded to a qualitative assessment. Therefore, an evaluation of the size of the crack propagation areas depending of the heat treatment conditions would be a very useful complement in further research.

## ACKNOWLEDGEMENTS

To CONACYT for the scholarships 1031303 and 773824 for Master and doctoral studies, respectively, and to TecNM by the support through the project 16909.23-P.

## REFERENCES

Abúndez, A., Pereyra, I., Campillo, B., Serna, S., Alcudia, E., Molina, A., Blanco, A., and Mayén, J. (2016). Improvement of ultimate tensile strength by artificial ageing and retrogression treatment of aluminium alloy 6061. *Materials Science and Engineering: A*, 668, 201–207. doi:10.1016/j.msea.2016.05.062.

ASTM International (2002). ASTM E466-96, Standard Practice for Conducting Force Controlled Constant Amplitude Axial Fatigue Tests of Metallic Materials. doi: 10.1520/E0466-21.

ASTM International (2004). ASTM E739-91. Standard practice for statistical analysis of linear or linearized stress-life (S–N) and strain-life (e–N) fatigue data. doi: 10.1520/E0739-10R15.

Azadi, M. and Shirazabad, M.M. (2013). Heat treatment effect on thermo-mechanical fatigue and low cycle fatigue behaviors of A356.0 aluminum alloy. *Materials Design*, 45, 279–285. doi:10.1016/j.matdes.2012.08.066.

Khonsari, M.M. and Amiri, M. (2012). *Introduction to Thermodynamics of Mechanical Fatigue*. CRC Press Taylor Francis Group, Boca Raton, FL. doi: 10.1201/b12725.

Mayén, J., Gallegos-Melgar, A., Mercado-Lemus, V., Hernandez-Hernandez, M., Abúndez, A., Alcudia, E., Pereyra, I., Serna, S., and Poblano-Salas, C. (2019). Control Parameters Correlation by Multiple Linear Robust Regression for the Design of Heat Treatments For Al-6063 Alloy. *Experimental Techniques*, 43(1), 91–103. doi:10.1007/s40799-018-0269-7.

Mayen, J., Gallegos-Melgar, A., Abúndez, A., Alcudia, E., Colín, J., and Barredo, E. (2019). Yield Strength Improvement of an Al-6063 Alloy by Applying a Novel Combination of Cold Working and Heat Treatments for Die Casting of Plastic Parts. *Transactions of the Indian Institute of Metals*, 72(5), 1211–1220. doi: 10.1007/s12666-019-01609-z.

Naderi, M., Amiri, M., and Khonsari, M.M. (2010). On the thermodynamic entropy of fatigue fracture. *Proceedings of the Royal Society A: Mathematical, Physical and Engineering Sciences*, 466(2114), 423–438. doi: 10.1098/rspa.2009.0348.

Naderi, M. and Khonsari, M. (2011). Real-time fatigue life monitoring based on thermodynamic entropy. *Structural Health Monitoring*, 10(2), 189–197. doi: 10.1177/1475921710373295.

Naderi, M. (2020). On the Evidence of Thermodynamic Self-Organization during Fatigue: A Review. *Entropy*, 22(3), 372. doi:10.3390/e22030372.

Nelaturu, P., Jana, S., Mishra, R.S., Grant, G., and Carlson, B.E. (2020). Effect of temperature on the fatigue cracking mechanisms in A356 Al alloy. *Materials Science and Engineering: A*, 780, 139175. doi: 10.1016/j.msea.2020.139175.

Petatan Bahena, K.E. (2022). *Evaluación del efecto de los tratamientos térmicos sobre la vida a fatiga de aleaciones de aluminio*. Master's thesis, TecNM/CENIDET, Cuernavaca, México.

Prigogine, I. (1978). Time, Structure, and Fluctuations. *Science*, 201(4358), 777–785. doi: 10.1126/science.201.4358.777.

Reed, R., Smith, J., and Christ, B. (1983). *The economic effects of fracture in the United States*, volume 647. US Department of Commerce, National Bureau of Standards. URL `https://www.govinfo.gov/app/details/GOVPUB-C13-831b1a5d974bb0b32ccfc5f0e249362c`.

Schütz, W. (1996). A history of fatigue. *Engineering Fracture Mechanics*, 54(2), 263–300. doi:10.1016/0013-7944(95)00178-6.

Teng, Z. (2023). Thermo-based fatigue life prediction: A review. *Fatigue Fracture of Engineering Materials Structures*, 46(9), 3121–3144. doi:10.1111/ffe.14079.